CFD Modelling of Leak of Liquid CO_2 from High Pressure Containments and subsequent Atmospheric Dispersion

Anjaneyulu Lankadasu[1], Amita Tripathi[2], Samuel Saysset[3], Angeles Yackow[3] and Bruno De La Roussiere[4]
[1]Fluidyn Consultancy (P) Ltd, 146, Ring Road, 5, HSR Layout, Bangalore - 560102, India
[2]Fluidyn France,7 Boulevard de la Liberation, Saint Denis-93200, France
[3]GDFSuez,361 avenue du Président Wilson, 93211 Saint-Denis La Plaine Cedex,France
[4]Entrepose Contracting,165 Boulevard de Valmy, Colombes-92700, France

In September 2012, DNV released the experimental datasets of two research projects conducted to investigate the potential hazards of accidental ruptures of pipelines transporting trans-critical CO_2. The transportation is often done via dedicated pipelines at high pressure (≥8 MPa), which has high risks of leaking or sudden ruptures. The present paper presents the results of the simulation of three cases among the ones that present the most extreme conditions of the DATASETS. The simulations are conducted in two separate stages: The first stage of the model takes into account the transition flow of supercritical CO_2 under the action of large pressure changes through small flow passages such as orifices. It considers steep changes in transport and thermodynamic properties using appropriate equations of state for the wide range of pressures involved and the second stage of the model calculates the large scale dispersion through the ambient air. This model includes consideration of the formation of dry ice due to sudden expansion and subsequent sublimation of dry ice due to entrainment of relatively hot ambient air. It also takes into account the effects of surrounding wind field using an atmospheric boundary layer model. The results have shown that calculated mass flow rate is within the devices accuracy (<11%). At the same time, the concentration and temperatures of CO_2 at several distances from the source are well represented by the simulation.

1. Introduction

CO2 emissions have been increasing over the years since the industrial revolution. It is widely accepted that its sequestration will be necessary to substantially reduce the global concentrations (Mazzoldi et al, 2012). Carbon capture and storage (CCS) could have a big impact on the global energy production, as it would decrease the emissions of fossil energy sources, still widely used around the planet (Global CCS Institute, 2009). The current technologies can potentially capture 80–95% of the CO2 emitted from an electric power plant or other industrial source. Sequestered CO2 could be then transported to places suitable for underground injection via high-pressure pipelines (Witlox et al, 2012). The transportation is often done via dedicated pipelines at high pressure (≥8 MPa), which has high risks of leaking or sudden ruptures. This kind of accidents may lead to a potential asphyxiation of the living ecosystem near the pipeline.

In order to investigate the potential hazards of this kind of ruptures, fill the identified knowledge gaps and to validate computer dispersion models for liquid and supercritical CO2 accidental releases, BP set up a research project in 2006 to identify those critical knowledge gaps that required to be filled (DNV CO2PIPETRANS JIP, 2006 and 2010). For this goal, an experimental program was developed and executed at the Spadeadam test site located in the North of England (Figure 1). A set of twelve CO_2 releases were delivered with CO_2 either in the liquid or supercritical state. Release pressures ranged from 82 – 159 barg, temperatures from 5 – 147 ˚C, and three orifice diameters were used, namely ¼", ½" and 1" (i.e. 65mm, 11.9mm and 25.6mm). Two of the releases were directed into an instrumented plate, two through an instrumented spool and one directed downwards onto the ground. From each release a comprehensive data set, photo library and video footage was obtained as well as considerable hands-on experience from working with a live CO_2 system.

The DATASET release 1 (DS1) document provides an overview of the test rig used during the BP research project as well as details on the nine releases that the CO2PIPETRANS released to the modelling community.

In 2010, Shell conducted a similar series of experiments at the Spadeadam test site with different conditions, eight datasets were released to the modeling community within the DATASET release 2 (DS2).

All eight datasets were recorded from horizontal releases of liquid and supercritical CO_2 within the pressure and temperature ranges of 80 – 150 barg and 0 – 70˚C, respectively, through orifice diameters ranging from ¼" to 1" (6.25mm to 25.4mm).

The physical process of the CO2PIPETRANS CO_2 release includes pressure drops to sub critical conditions and phase change within the short tube orifice (release nozzle). Further, at the downstream of the nozzle, the fluid rapidly expands to atmospheric pressure and this could lead to dry ice formation. Subsequently, the dry-ice could sublimate after gaining heat from ambient air, or rain out as big drops and deposit on the ground. The whole process scenario primarily depends on the initial pressure and temperature of the reservoir (storage tank).

The present paper covers the validation of discharge and dispersion results obtained by a generalized 3D CFD based model against the experimental results of 3 steady state cases of CO2PIPETRANS.

Nomenclature

A	leak area
C_{pl}	liquid specific heat at constant pressure at saturation condition, J/(kg K)
h_g, h_s, h_t	specific enthalpy of gas, solid and mixture, respectively, J/kg
h_{sg}	difference between specific enthalpies of gas and solid, J/kg
L	latent heat of evaporation, J/kg
S_e	evaporation source term in the scalar equation, kg/m^3
T	fluid temperature, K
T_{sat}	saturation temperature, K
y_g, y_s	mass fraction of gas and solid, respectively
ρ_l	liquid density at saturation condition, kg/m^3

2. Description of experimental conditions for leak and dispersion

Three representative cases, from both DATASETS, are selected for validation. Operating conditions of the three cases are summarized in Table 1. These cases have been selected as they present the most extreme conditions among all of the operational conditions conducted by the CO2PIPETRANS project (DNV CO2PIPETRANS JIP, 2006 and 2010). Therefore, they represent a simulation challenge to be validated.

For instance:

From DATASET1 (BP)

- T5: Biggest release diameter, there could be solid formation as it is a cold release

- T8: Transient release

- T11: Cold release chosen as the first validation case

From DATASET2 (Shell)

- T11: cold liquid release, for these conditions, there is high probability of dry ice formation

3. Model implementation

3.1. Computational domain and boundary conditions

Schematic diagram of the computational domain considered for discharge simulation is shown in Figure 2. Reservoir is considered as an equivalent volume axis-symmetric pipe. Although the pressure lose at the entrance of hose from the reservoir is small compared to the entrance of the orifice from hose, for low mass flow rate cases, the same kind of computational domain is used for all cases with respective dimensions. Initially the domain is filled with CO_2 at operating pressure and temperature. Because of pressure difference between orifice and ambient, velocity field developed until chocked flow conditions reached.

The boundary conditions are the following:

- **Inlet:** pressure static with effective distance is equal to zero and operating temperature, to mimic the constant operating pressure in the reservoir. It is represented by the violet line on Figure 2
- **Exit:** pressure static with effective distance is equal to zero; pressure at the exit is fixed to ambient pressure. It is represented by the light blue line on Figure 2

- **Wall:** Non-slip and adiabatic. . It is represented by the dark blue line on Figure 2
- **Symmetric:** On all remaining boundary faces

Figure 3 shows the computational domain and mesh distribution in the domain. The parameters used are shown in Table 2.

3.2. Numerical model

To solve both the discharge and dispersion problems the three dimensional Navier-Stokes equations along with scalar transport equations are solved using an implicit, pressure based, finite volume method for non-uniform unstructured mesh. Turbulence is modelled using a two equation model. Thermodynamic and transport properties of CO_2 are calculated such that the steep variations in them near the pseudo-critical are properly considered.

Phase change: liquid to vapor

To model the two phase flow and phase change across the leak that occurs during the release, homogeneous equilibrium model (HEM) is used. In this model it is assumed that the velocity and the temperature of all the phases are same. In the present simulation, energy equation is solved in the form of total enthalpy instead of static temperature. In general, the actual two phase flow of CO_2 is non-homogeneous and non-equilibrium. However, the ratio of vapor and liquid velocities and inter-face velocity differences between two phases (slip) is expected to be small in this case (DNV CO2PIPETRANS JIP, 2006 and 2010). Further, the density ratio of liquid to vapor near the critical point is almost equal to unity and this ratio is good indication of insignificant slip between the phases (Zhang and Yang, 2005). Therefore, the HEM is selected to model the two phase flow. For a particular temperature and pressure, a point on the phase diagram is defined and all the relevant properties are calculated. If the control volume containing the specified point is occupied by both liquid and vapor, they are supposed to be in equilibrium. Hence the point always lies on saturation line. If, on the other hand, the temperature and pressure in a specified control volume is away from the saturation line, then the corresponding saturation temperature (at constant pressure) is calculated. The difference in the temperature is the driving potential for phase change. Then using this temperature difference and the specific heat of liquid, density of saturated liquid and latent heat of evaporation, the amount of liquid to be evaporated is calculated as in Equation 1and is added as the source term for the scalar equation.

$$S_e = \frac{\rho_l \left(T - T_{sat}\right) C_{pl}}{L} \tag{1}$$

Phase change: solid (dry-ice) to vapor

Mass fraction of dry ice (solid CO_2) after expansion to the ambient is obtained from the pseudo source point calculation. Though the mass fraction of the dry ice is significant, volume fraction of dry ice is very low. Further, particle size of dry ice is observed to be a few microns. Hence, the spatial distribution of dry ice is obtained by solving a scalar transport equation. It is considered while calculating the mixture density.

3.3. Coupling between discharge and dispersion simulations

Because of chocked flow condition, pressure is above the ambient pressure at the exit of the orifice and hence the expansion in the downstream results in a series of shock and expansion waves. The time and length scales of these waves are quite small compared to the dispersion time and length scales. Hence resolving such kind of flow behaviors in dispersion domain is computationally expensive and gives trivial benefits as far as dispersion is considered. Therefore, it is very much beneficial to use dispersion source point, called pseudo source, (Fauske HK and Epstein, 1988) at which the pressure of the jet reaches ambient.

In the present study, discharge and dispersion simulations are carried out in two different CFD based softwares, namely fluidyn-MP for discharge and fluidyn-PANACHE for dispersion. The discharge simulation software has been tuned with the models developed on (Bae et al, 2005), in order to have a high accuracy on its results. At the same time, fluidyn-PANACHE, has been already used in the past to validate dispersion results for CO2 releases (Henk et al, 2012).

In the discharge stage, the domain is considered only up to exit of the orifice. Since the pressure at the exit of the orifice in the discharge simulation is not equal to the ambient pressure, the state of the fluid could be pure liquid, pure vapor or a mixture of liquid and vapor phase depending on the orifice size and condition inside the pipe.

To feed the exit data as source for the dispersion simulation (in fluidyn-PANACHE), mass flow rate, temperature and velocity are calculated at ambient pressure. To achieve that, instantaneous flashing assumption is invoked. According to this assumption, total enthalpy before flashing and after flashing will remain constant. Because of that constraint, at ambient pressure, the state of the fluid would be either pure vapor or mixture of dry-ice and vapor depending on initial total enthalpy of the fluid. Again, that total enthalpy value depends on temperature and pressure of the reservoir. For a given ambient pressure, sublimation temperature can be calculated. Hence, the inlet temperature is fixed at sublimation temperature corresponding to ambient pressure.

The following assumptions are made while deriving the pseudo source point:

- No entrainment of surrounding ambient air, because the pressure of the jet is higher than ambient pressure.
- Lateral velocity gradients and diffusion are negligible in the momentum equation.

- No heat transfer between the jet and ambient, hence total enthalpy is constant.
- Discharge from the leak is a mixture of liquid and vapor and at source point the mixture contains only vapor and solid ice.
- At the pseudo source point sublimation temperature is fixed to 194K corresponding to the ambient pressure of one atmospheric.

Velocity, area and the composition of the flashed jet at the pseudo-source point for dispersion are calculated using the following 1D mass, momentum and energy conservation equations:

$$A_3 = \left(\frac{\rho_2 A_2 u_2}{\rho_3 u_3} \right) \tag{2}$$

$$u_3 = u_2 + \left(\frac{p_2 A_2 - p_3 A_3}{\rho_2 u_2 A_2} \right) \tag{3}$$

$$h_{t2} = h_{s3} + y_{g3} h_{sg3} + 0.5 u_3^2 \tag{4}$$

In Eq. 2 to Eq. 4, subscript 2 denotes the exit of the leak and subscript 3 denotes the location where the pressure of the jet reaches the ambient pressure. The distance between 2 and 3 is not known from any of the above equations. According to experimental observation, it could be anywhere between 10 to 15 times of the orifice diameter. This distance is negligibly small compared to overall dimensions of the dispersion domain. The most important inherent assumption is that the pressure at the pseudo source point is equal to the ambient pressure, which further fixes the sublimation temperature to 194K.

4. Results

4.1. Mass flow rate through a short-tube orifice

To validate the CFD model for transition flow through small leaks the numerical results are compared with the experimental measurements of mass flow rates through a short tube orifice (Liu et al, 2004; Zhang and Yang, 2005). An orifice of diameter is 1.35 mm and length 12.92 mm is fixed in a pipe of diameter 7.03 mm. Table 3 shows the comparison of mass flow rates. It is found that the current CFD model is able to calculate the pressure variations and mass flow rates reasonably well for different conditions.

Comparison of predicted pressure profiles along the orifice centerline (axis) with experimental values is shown in Figure 4. The pressure oscillations at the exit of the orifice are due to the sudden expansion of the flow to surrounding pressures. These oscillations could be attributed to partially resolved shock and expansion waves. Further, intensity of oscillations decreases with reduction in the inlet pressure. Accurate calculation of the pressures, lead to accurate calculations of the mass flow rate at the orifice exit. The calculated pressure profiles and the experimental results are in good agreement (Figure 4). The maximum pressure deviation in the orifice compared to the experimental pressure values is around 10% for the 7.52MPa pressure case.

4.2. Mass flow rate from the high pressure CO_2 tank through the orifice

Once the difference of pressure between the entry and the exit is big enough, the mass flow rate is only a function of inlet pressure regardless of the exit pressure (Zhang and Yang, 2005) this is known as choked flow. Thus, accurate calculation of the mass flow rate is critical for a CO_2 release, as it is the main variable for dispersion simulations and its calculation does not depend on the atmospheric pressure, but mainly on the pressure and temperature inside the reservoir for a given orifice. In the present study both steady and transient releases are considered. For steady release cases, reservoir is maintained at constant pressure and temperature using a buffer gas. Because of that mass flow rate is uniform throughout the discharge duration. Hence, numerical simulations are carried out in steady state mode whereas for transient release there is no buffer gas. Consequently pressure inside the reservoir decreases with time and in turn mass flow rate also decreases with time. The reservoir pressure for all these cases is above thermodynamic critical pressure, but the temperature is below thermodynamic critical temperature. Therefore, thermodynamic state of the fluid in the reservoir is dense liquid. For cases T11DS1 and T11DS2, the diameter of the orifice, the reservoir pressure and the exit pressure are the same, but the reservoir temperature is different, 18°C higher for case T11DS1. Therefore, the vapor fraction will be bigger in the first case leading to a smaller pressure drop across the orifice.

First this model was tested with the steady state scenarios. Comparison of mean mass flow rate is shown in Table 4. Overall, simulation results agree with the experimental results within the maximum error in the mass flow rates obtained from the experimental data (±20%) (DNV CO2PIPETRANS JIP, 2006 and 2010). For the case of high mass flow rate, numerical prediction is higher than the experimental measurement whereas for low mass flow rate cases, it is under predicted. For high mass flow rate scenario, losses due to higher-pressure drops in the connecting hose could have a higher effect on the mass flow rate than the heat transfer. On the other hand, for low mass flow scenario, compared to frictional losses in the connecting hose, heat transfer through the walls of the hose and orifice could be significant. Given that, no experimental details were given about the heat transfer on this zone (kind of insulation, pipe heat conduction, etc.), further improvement would need more details and measurements.

Variation of mass flow rate with time is compared with the experimental data and shown in Figure 5. Disagreement of computed mass flow rate with the measurement during the initial transient could be attributed to the variations in the actual operating conditions from those reported. For example, the temperature of the reservoir was expected to be constant by supplying heat through the heaters attached to the reservoir pipe. However, the experimental measurements of reservoir temperature show some variations with time (DNV CO2PIPETRANS JIP, 2006 and 2010). For the present simulations, the assumption of an adiabatic wall invoked. In addition, there is heat transfer from hot CO_2 to cold ambient air, through the flexible hose and orifice. In reality, this equipment is at ambient temperature before experiment starts. Nevertheless, in the simulations, these walls also are assumed as adiabatic. This affects the effective temperature of the CO_2 flowing through the orifice, hence, it could be smaller in the experiments. Overall, the deviation of computed flow rates from the measurement is within the experimental error, which is about 20% (DNV CO2PIPETRANS JIP, 2006 and 2010).

4.3. Dispersion of leaked CO_2 to the ambient

Figure 6 shows the computational domain and mesh for the numerical simulation of the dispersion of the leaked CO_2 into the surrounding air. To capture the turbulence generation by obstacles on the test site, large scale obstacles are resolved on the computational mesh. The ground is treated as smooth because of concrete base and the effect of different kinds of probes and their stands are not modeled. To resolve the high momentum jet near the source, nested domain with fine mesh has been generated around the source. In order to solve with high accuracy the temperature variations near the source point, a small mesh size would be needed. Hence, in order to decrease the simulation time, while keeping good accuracy, a pseudo source was used. This means that, for cold releases in which there is a high probability of dry-ice formation, the temperature is fixed at sublimation temperature of 194.16K corresponding to ambient pressure. In reality, the temperature changes according to local pressure, in addition, near the injection the experimental measurements show that pressure is usually smaller than ambient pressure. The local pressure controls the minimum temperature of the jet in case of cold release; hence, there is a possibility of dry ice formation if local pressure is lesser than sublimation pressure.

Table 5 compares CO_2 volume fraction for steady state cases with experimental measurements. Experimental results have an implicit noisy variation, which is increased far from the source. Even for steady cases, the concentrations reported by the sensors vary with time. On the other hand, for steady simulations there is only a unique value at converged state for each point. The experimental measurements and simulation results are in good agreement and within the range for each sensor. Detailed description of the results and comparison is given in Lankadasu et al (2014).

The volume fractions of CO_2 at different distances from the leak for the transient case of T8DS1 are shown in Figure 7. Volume fraction of CO_2 into the dispersion domain at the point source is one. There is little chance to entrain air into the CO_2 jet front other the mere diffusion. Because of this concentration of CO_2 during early transient is high and slowly decreases with time. Because of three-dimensional transient simulation, running for large transient could be expensive and in many times it could not require drawing typical conclusion from simulation results. Therefore, the simulation was stopped at 70s whereas experimental measurements were collected for ~120s. Overall, the concentration profiles are found to closely agree with the experimental measurements.

Most of the expansion of leaked CO_2, and hence property changes occur in a short time span, which complicates the simulation process. Nevertheless, the assumption of a pseudo source point had shown that the concentration along the jet centerline is in fairly good agreement with the experimental measurements for both steady and transient cases. To get better comparison close to the leak, it would have been needed a finer mesh between 0 and 1m from the source, however, the CPU time would have been greatly increased. In general, the concentration is well predicted within the uncertainties of the experimental measurements.

5. Conclusions

A 3D CFD based model is developed to study flow of CO_2 under large variations in pressure. It is found that the developed model is able to handle the transition of flow from supercritical or high pressure liquid regimes through the two-phase liquid-vapor regime to the completely vapor state. The model is validated by comparing mass flow rates under different conditions. It is found that the deviations in computed mass flow rates are within the experimental error. In general, the fluid at the exit of the orifice is found to be a mixture of liquid and vapor. Further, the same model was extended to study the expansion of high pressure CO_2 to the ambient air and its subsequent dispersion. Formation, and sublimation, of the solid CO_2 (dry ice) in the post-expansion zone is captured and it affects the temperature immediately after the orifice exit. The computed CO_2 concentrations match reasonably well with the measurements for different scenarios.

Acknowledgements

The authors thank CITEPH (Concertation pour l'Innovation Technique pour l'Exploration et la Production des Hydrocarbures), GDFSuez and ENTREPOSE Contracting for the support given to this project.

References

1. Bae, J. H., Yoo, J. Y. and Choi, H., 2005, Direct numerical simulation of turbulent supercritical flows with heat transfer, Phys. Fluids, Volume 17, 105104.

2. DNV CO2PIPETRANS JIP- data release 1 – Advantica overview r01_tcm4-520088 (http://www.dnv.com/industry/oil_gas/services_and_solutions/technical_advisory/process_integrity/ccs_carbon_capture_storage/co2pipetrans/co2pipetrans_data_form.asp)

3. Fauske, H. K. and Epstein, M., 1988, Source term considerations in connection with chemical accidents and vapour cloud modelling. J Loss prev Process Ind, 1:75-83.

4. Global CCS Institute, Strategic Analysis of the Global Status of Carbon Capture and Storage. Final Report: Existing CCS Research and Development Networks around the World. The Global CCS Institute, Camberra, Austrlia (2009).

5. Lankadasu, A., Tripathi, A., Saysset, S., Yackow, A. and De La Roussiere, B. (2014) Numerical modeling of supercritical CO_2 leaks and its subsequent dispersion in the ambient air, IUTAM Symposium on Multiphase flows with phase change: challenges and opportunities, Hyderabad, India, Dec 08–11.

6. Liu, J. P, Niu, Y.M., Chen, J.P., Chen, Z.J. and Feng, X., 2004, Experimentation and correlation of R744 two-phase flow through short tubes. Exp Therm Fluid Sci, 28:565.

7. Mazzoldi, A., Picard, D. and Oldenburg, C. M., 2012, Simulation-based estimates of safety distances for pipeline transportation of carbon dioxide. Greenhouse Gas Sci Technol. 2:1–18.

8. Witlox, H. W. M, Harper, M. and Oke, A., 2012, Phast validation of discharge and atmospheric dispersion for pressurised carbon dioxide releases. Hazards XXIII. SYMPOSIUM SERIES NO. 158

9. Zhang, C.L. and Yang, L., 2005, Modeling of supercritical CO2 flow through short tube orifices. J Fluids Eng,127:1194.

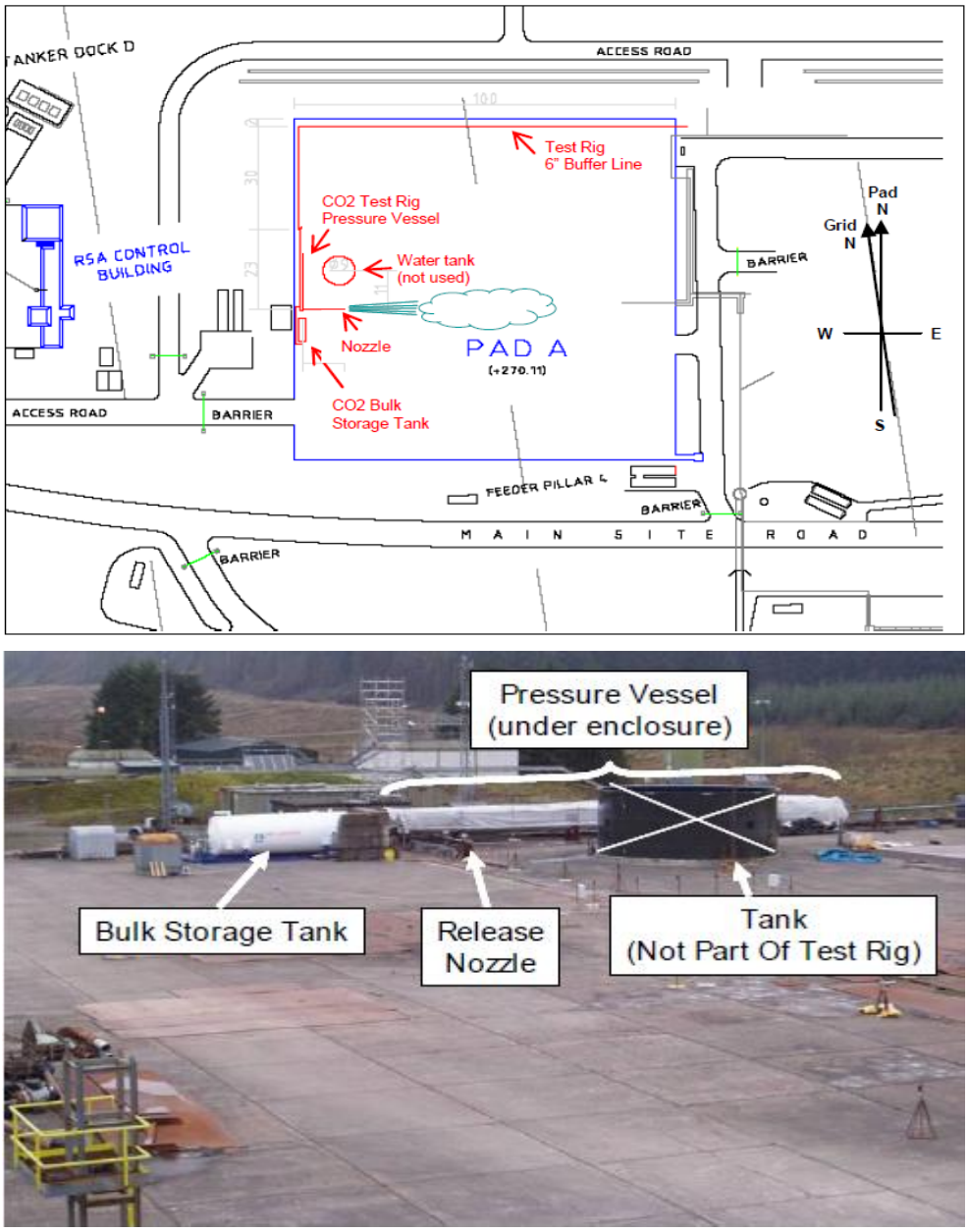

Figure 1 : Spadeadam site map. The Pad A is the zone in which the tests were conducted

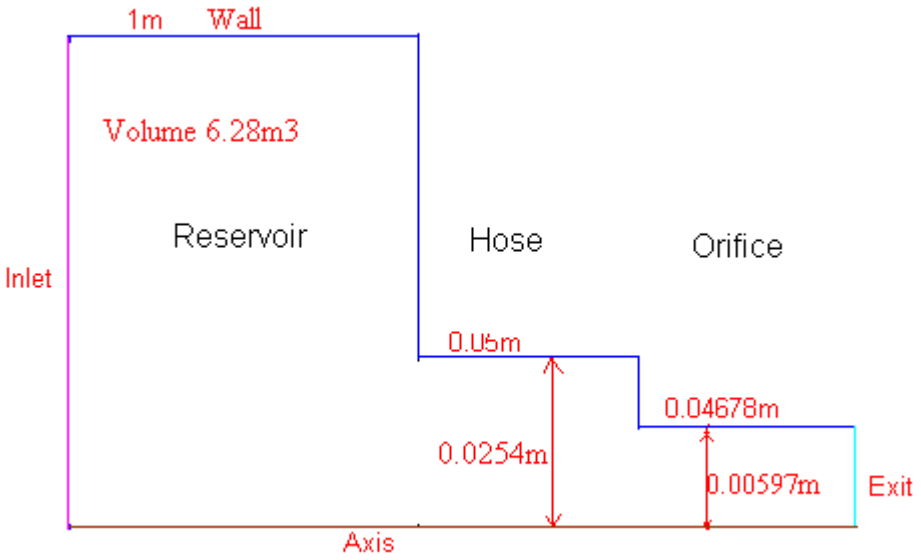

Figure 2: Dimensions of the release nozzle

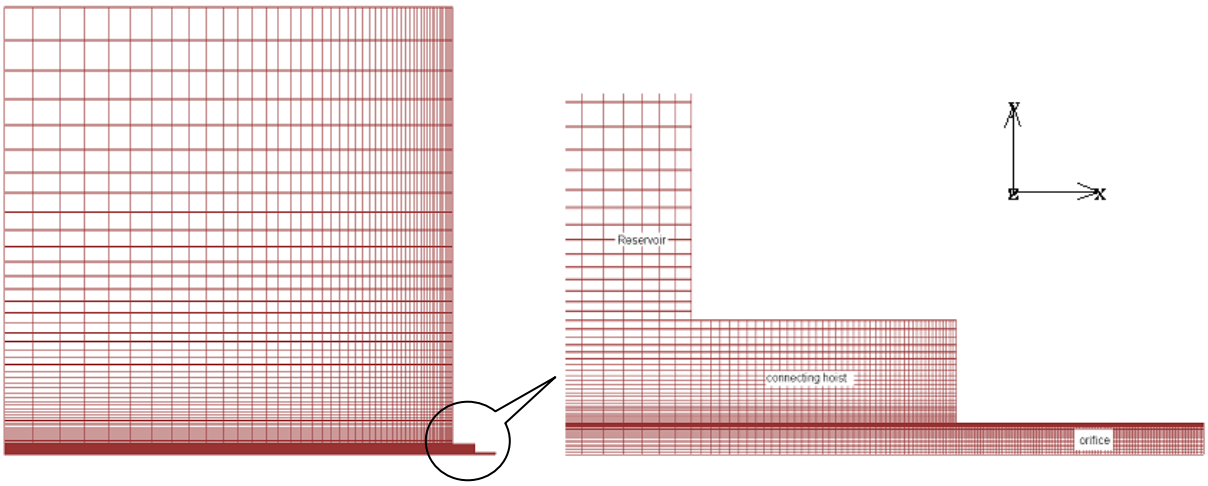

Figure 3 : Mesh distribution on the selected computational domain

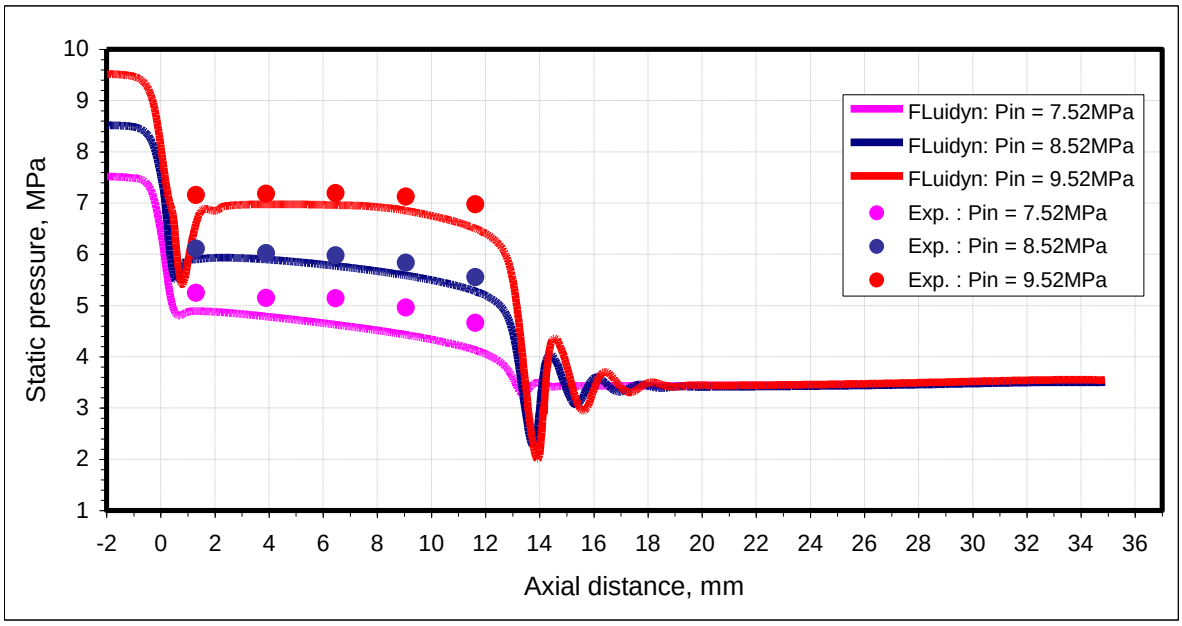

Figure 4. Static pressure plot along the centre line: Inlet pressure, (a) 7.52Mpa, (b) 8.52Mpa, (c) 9.52Mpa. Experimental data is taken from Liu et al (2004)

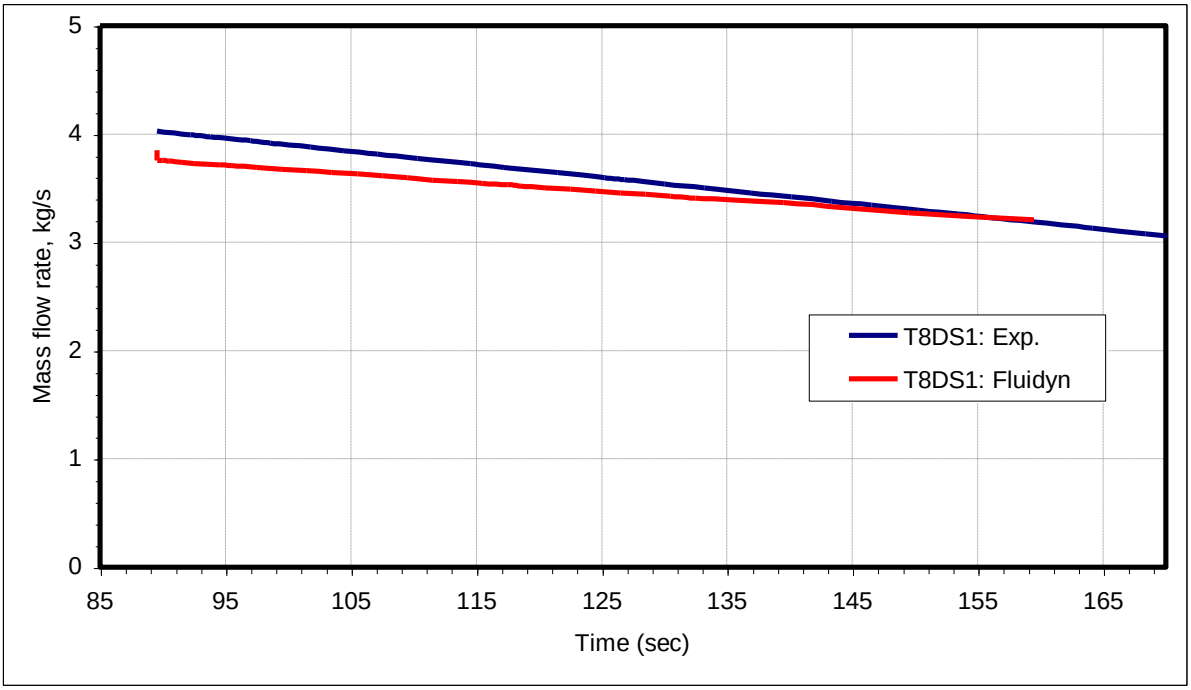

Figure 5. Comparison of mass flow rate predicted by simulation with experimental results

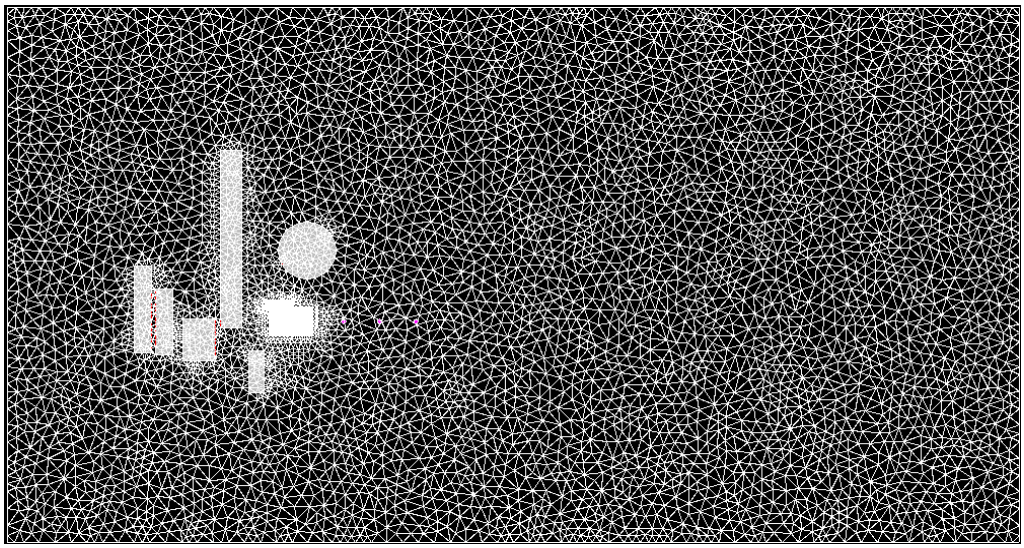

Figure 6. Computational domain and mesh for dispersion domain

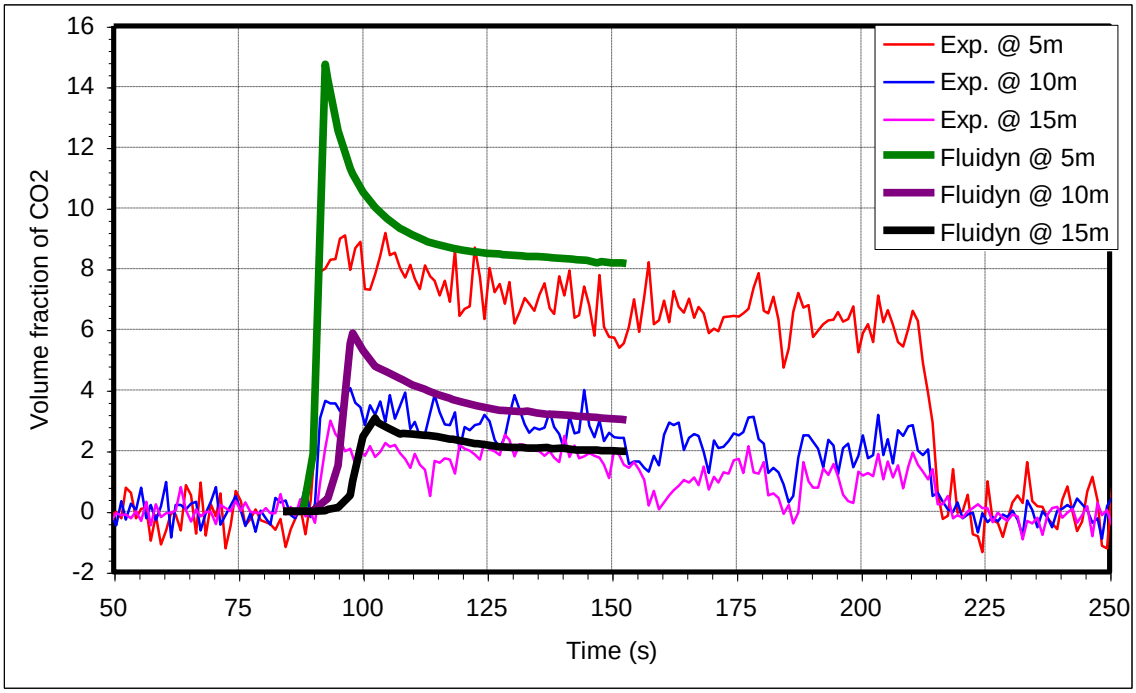

Figure 7. Comparison of CO_2 volume fraction predicted by simulation with experimental results

Table 1: Summary of experimental conditions for CO2PIPETRANS cases

Discharge data	DATA SET 1		DATA SET 2
	T5	T11	T11
Inlet pressure (bar)	156.9	82.2	81.9
Inlet temperature (°C)	12.5	18.4	-0.2
Orifice diameter (mm)	25.4	12.7	12.7
Orifice length (mm)	72.41	46.78	46.78
Orientation	horizontal	horizontal	horizontal
Ambient pressure (bar)	0.9854	0.9602	0.995
Ambient temperature (°C)	5.8	11.6	3.6
Mean mass flow rate (kg/s)	40.7	7.1	9.0
Wind direction (°)	278.6	270.8	261

Table 2: Parameters used for simulation

Total volume of the reservoir (m^3)	6.3
Total mass of the CO2 at initial conditions (kg)	1502
Grid type	Structured orthogonal non-uniform grid
Turbulence model	k-ε

Table 3. Comparison of mass flow rates for flow through a short-tube orifice

Upstream pressure (MPa)	Upstream temperature (K)	Downstream pressure (MPa)	Computed mass flow rate (kg/hr)	Measured mass flow rate (kg/hr)	% error
7.52	308.36	4.66	109.8	118	-6.94
8.52	308.36	5.55	177.9	168	5.89
9.52	308.36	6.97	231.7	225	2.98

Table 4. Comparison of calculated mass flow rate with experimentally measured value

Case	Reservoir pressure, bar	Exit pressure, bar	Reservoir temperature, °C	Predicted mass flow rate, kg/s	Measured mass flow rate, kg/s	Percentage deviation, %
T5DS1	156.9	0.9854	12.5	45	40.7	10.6
T11DS1	82.2	0.9602	18.4	6.4	7.1	-9.9
T11DS2	81.9	0.995	-0.2	8.1	9	-10.0

Table 5. Comparison of dispersion results with experiment for steady state cases

Case	Distance from source, m	Volume fraction of CO_2, %		Temperature, °C	
		Simulation	Experiment	Simulation	Experiment
T5DS1	20	5.18	6.6 ± 4	-15.06	-14.5 ±10
T11DS1	5	11.72	18.16 ± 4	-40.31	-
T11DS2	5	13.12	15	-50.43	-52